ELSEVIER

Journal of Power Sources 68 (1997) 524–529

JOURNAL OF POWER SOURCES

Electrochemical lithium intercalation into and de-intercalation from porous $LiCoO_2$ electrode by using potentiostatic current transient technique

Su-Il Pyun *, Young-Min Choi

Department of Materials Science and Engineering, Korea Advanced Institute of Science and Technology, 373-1 Kusong-Dong, Yusong-Gu, Daejon 305-701, South Korea

Accepted 28 October 1996

Abstract

The lithium-ion transport through a porous $LiCoO_2$ electrode in 1 M $LiClO_4$/propylene carbonate (PC) solution was investigated by using cyclic voltammetry, galvanostatic intermittent charge/discharge experiments and potentiostatic current transient techniques. The apparent chemical diffusivities of the lithium ion were determined as a function of the lithium charging potential during lithium intercalation and de-intercalation. In the lithium charging potential range, not less than the plateau potential with intensive intercalation/de-intercalation, both the cathodic and the anodic current transient curves obtained from the porous oxide electrode are divided into two stages. The first stage is due to the diffusion of the lithium ion through the oxide electrode and the second stage is associated with the accumulation of the lithium ion at the center of the oxide particle. During lithium intercalation, the time from the first to second stage transition decreased with decreasing lithium charging potential. This suggests that the lithium-ion transport during the intercalation proceeds not by the diffusion in a single phase, but by the diffusion-controlled movement of boundary between a concentrated β-phase and a dilute α-phase. The apparent chemical diffusivity of the lithium ion in the porous oxide electrode was determined to be (10^{-9}–10^{-8}) $cm^2\ s^{-1}$ at room temperature. During the lithium de-intercalation, the apparent chemical diffusivity decreased with decreasing lithium charging potential. The reduced diffusivity value is attributable to a raised lithium content in the oxide electrode. By contrast, during the lithium intercalation the apparent chemical diffusivity increased with decreasing lithium charging potential. The exact opposite dependencies of the lithium-ion diffusivity on the lithium charging potential during the intercalation and de-intercalation were discussed in terms of the phase-boundary movement which is caused by the intercalation-induced stress gradient developed across the α/β-phase boundary. © 1997 Elsevier Science S.A.

Keywords: Porous electrodes; Lithium transport; Chemical diffusivity; Current transient; Phase-boundary movement; Lithium cobalt oxides

1. Introduction

The electrochemical lithium intercalation reaction into transition metal oxides has been studied by many researchers [1–3] due to their versatile applications in the cathode material for high energy density rechargeable batteries and electrochromic display devices. The intercalation reaction is described as a reversible insertion of guest species into a host lattice without significant structural modification of the host.

The term 'intercalation materials' has been used for a large group of compounds which incorporate a large range of guest species and show a wide variability of chemical and physical properties. Recently, a more advanced rechargeable lithium battery system called the 'lithium-ion cell' or 'rocking-chair cell' has been developed by using the intercalation materials as the electrodes [4]. This employs strongly oxidizing compounds capable of reversibly intercalating lithium ion above 4 V_{Li/Li^+} as the cathode materials. Transition metal oxides such as $LiCoO_2$ [5], $LiNiO_2$ [6], $LiNi_{1-y}Co_yO_2$ [7], and $LiMn_2O_4$ [8] are known to satisfy this requirement.

Since electrochemical lithium intercalation and de-intercalation are in general limited by the rate of lithium diffusion through the oxide electrode, previous works [9,10] were focused on the determination of lithium diffusivity in the electrode material.

In general, lithium intercalation is accompanied by a molar volume change and, hence, the generation of the mechanical

* Corresponding author. Tel. (82) 42-869-3319; Fax: (82) 42-869-3310; e-mail: sipyun@sorak.kaist.ac.kr

PII S0378-7753(96)02631-6

stress gradient over the oxide particle [11]. The intercalation-induced stress gradient developed across the oxide powder electrode may give rise even to the formation of an intercalated lithium-concentrated phase. Once the new phase is formed, the lithium-ion transport through the oxide electrode may proceed by the phase-boundary movement rather than the diffusion of the lithium ion. The effect of phase-boundary movement on the lithium-ion transport through the porous oxide electrode is not yet elucidated. Therefore, the current transient analysis of the phase-boundary movement should give a better understanding of the lithium-ion transport through the $LiCoO_2$ electrode as an innovative rechargeable battery system.

This work involves the lithium-ion transport through the porous $LiCoO_2$ electrode by using a potentiostatic current transient method supplemented by cyclic voltammetry and galvanostatic intermittent charge/discharge experiments. The apparent chemical diffusivity of the lithium ion in the porous oxide electrode was determined as a function of the lithium charging potential by potentiostatic current transient techniques. The variation of the apparent chemical diffusivity with lithium charging potential was discussed in relation to the diffusion-controlled movement of boundary separating the two phases.

2. Experimental

$LiCoO_2$ powder was prepared by calcination of a pressed mixture of Li_2CO_3 and $CoCO_3$ at 600 °C for 6 h in air, followed by heating at 850 °C for 24 h in air with intermittent grindings. The resulting powder specimen was ground to below 10 μm in particle size through ball milling. The crystal structure of $LiCoO_2$ was characterised by X-ray diffraction (XRD). Powder XRD pattern was recorded on an automated Rigaku powder diffractometer using Cu Kα radiation. The porous electrode specimen was prepared by mixing $LiCoO_2$ powder with 5 wt.% Vulcan XC-72 carbon black and 2 wt.% poly(vinylidene fluoride) (PVDF) which was used as the working electrode.

A three-electrode electrochemical cell was employed for the electrochemical measurements. The reference and counter electrodes were constructed from lithium foil and a 1 M $LiClO_4$/PC solution was used as the electrolyte.

Galvanostatic intermittent charge/discharge curves were obtained under a constant-current condition by using an EG&G PARC Model 263A potentiostat/galvanostat. The charge and discharge currents were selected so that a change in lithium content of $\Delta\delta = 1$ for $Li_{1-\delta}CoO_2$ would occur for 5 h. A cyclic voltammogram was measured on the porous $Li_{1-\delta}CoO_2$ electrode with a scan rate of 0.01 mV s^{-1} in the potential 3.1–4.5 V_{Li/Li^+} range.

Potentiostatic current transient tests were performed on the porous oxide electrode as a function of the lithium charging potential in the potential 3.0–4.1 V_{Li/Li^+} range for 5000 s. Prior to the lithium intercalation, the electrode was maintained at 4.2 V_{Li/Li^+} for 3000 s. Subsequent potentiostatic lithium de-intercalation from the oxide electrode was made at 4.2 V_{Li/Li^+} for 7500 s.

All the electrochemical experiments were usually performed at 25 °C in a glove box (VAC HE493) filled with purified argon gas.

3. Results and discussion

Fig. 1 presents the cyclic voltammogram obtained from the porous $LiCoO_2$ electrode at 25 °C. The strong reduction and oxidation current peaks appeared noticeably at the potentials of 3.90 and 4.05 V_{Li/Li^+}, respectively, due to the intercalation of the lithium ion into and de-intercalation from the intercalation sites in the oxide structure available for the lithium ion.

The $LiCoO_2$ phase (referred to as high temperature-$LiCoO_2$, HT-$LiCoO_2$) prepared in this study has a hexagonal structure with a $R\bar{3}m$ space group. In contrast, the $LiCoO_2$ phase (referred to as low temperature-$LiCoO_2$, LT-$LiCoO_2$) synthesised at 400 °C shows a spinel-like structure with a $Fd3m$ space group [12,13].

The cyclic voltammogram in Fig. 1 indicates that the Li/HT-$LiCoO_2$ half-cell clearly undergoes a single-stage reduction of the lithium ion and oxidation of lithium. This behaviour can be accounted for by the fact that lithium ions are located only at the octahedral sites in the HT-$LiCoO_2$. In contrast, lithium ions are located at the tetrahedral sites as well as the octahedral sites in the LT-$LiCoO_2$ [14].

The two weak current peaks additionally occurred at 4.28 and 4.31 V_{Li/Li^+} higher than the intercalation/de-intercalation peak. The two slightly small peaks are presumably assigned to the order/disorder phase transition arising at $(1-\delta)$ 0.45 to 0.5 in the HT-$Li_{1-\delta}CoO_2$ [15]. The isother-

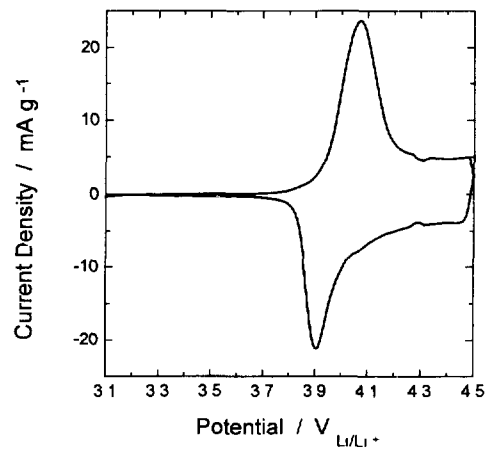

Fig. 1. Cyclic voltammogram obtained from the porous $LiCoO_2$ electrode in 1 M $LiClO_4$/PC solution at 25 °C, scan rate: 0.01 mV s^{-1}.

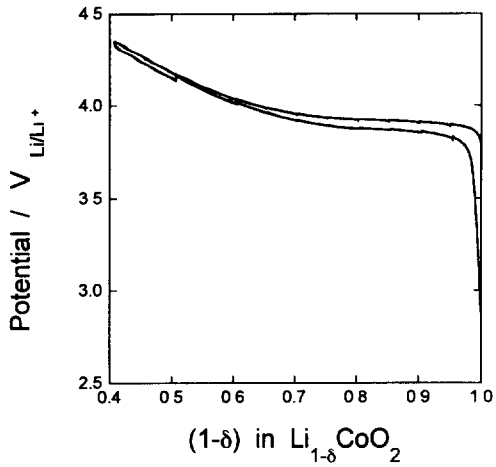

Fig. 2. First galvanostatic intermittent charge/discharge curve for the cell Li/1 M $LiClO_4$/PC/porous $Li_{1-\delta}CoO_2$ electrode at 25 °C; charge/discharge: 5 h rate.

mal order/disorder transition ran with progressively stronger and more widely spaced (in V_{Li/Li^+}) peak as the cell temperature is lowered from 25 to 10 °C.

Fig. 2 shows the first galvanostatic intermittent charge/discharge curves of the porous $LiCoO_2$ electrode in 1 M $LiClO_4$/PC solution at 25 °C in the intercalated lithium content, $(1-\delta)$, ranging from 0.4 to 1.0. The deviation from the ideal stoichiometry of $LiCoO_2$, δ, was calculated from the values of the mass of the oxide and the electrical charge that was transferred during the application of current pulses. The charge/discharge curve displays a wide potential plateau near 3.95 V_{Li/Li^+} in the $(1-\delta)$ range from 0.7 to 1.0. The occurrence of the plateau is due to the coexistence of two pseudo-phases of an Li-dilute α-phase and an Li-concentrated β-phase [16]. The intercalation/de-intercalation proceeds to a greater extent in the potential range greater than or equal to the plateau potential 3.95 V_{Li/Li^+}.

The electrochemical intercalation reaction is affected by various factors such as mechanical stress, phase transformation, and electric field generated during the intercalation of the lithium ion. The application of a large potential step or a current pulse to the electrode material may cause a very steep concentration gradient of the intercalated lithium ion and at the same time a large stress gradient near the surface region of the oxide electrode. The intercalation-induced stress is associated with the coherency stress required to hold together phases with different lattice parameters and may give rise even to the formation of the intercalated lithium-concentrated β-phase. Hence, the enhancing or impeding effect of the intercalation-induced stress on the lithium-ion transport during the lithium intercalation/de-intercalation is expected to appear more markedly in lower lithium charging potential range.

Fig. 3(a) and (b) presents the potentiostatic cathodic and anodic current transient curves in logarithmic scale, respectively, obtained from the porous $LiCoO_2$ electrode in 1 M $LiClO_4$/PC solution at various lithium charging potentials, as indicated in the figures. At lithium charging potentials greater than or equal to the plateau potential in Fig. 2, both the cathodic and the anodic current transients were divided into two stages. The first stage is due to the lithium-ion diffusion through the oxide electrode and the second stage relates to the accumulation of the lithium ion at the center of the oxide particle [17]. On the other hand, as the lithium charging potential is dropped to 3.8 V_{Li/Li^+} or less than 3.8 V_{Li/Li^+}, the potentiostatic cathodic current transients were composed of more than two stages.

The values of the transition time t_{tr} were measured as the time at which the slope of the current transient begins to deviate from the initial value. From Fig. 3(a) it is seen that during lithium intercalation t_{tr} decreased with decreasing lithium charging potential, i.e., as the concentration gradient across the oxide particle near the electrolyte/oxide electrode

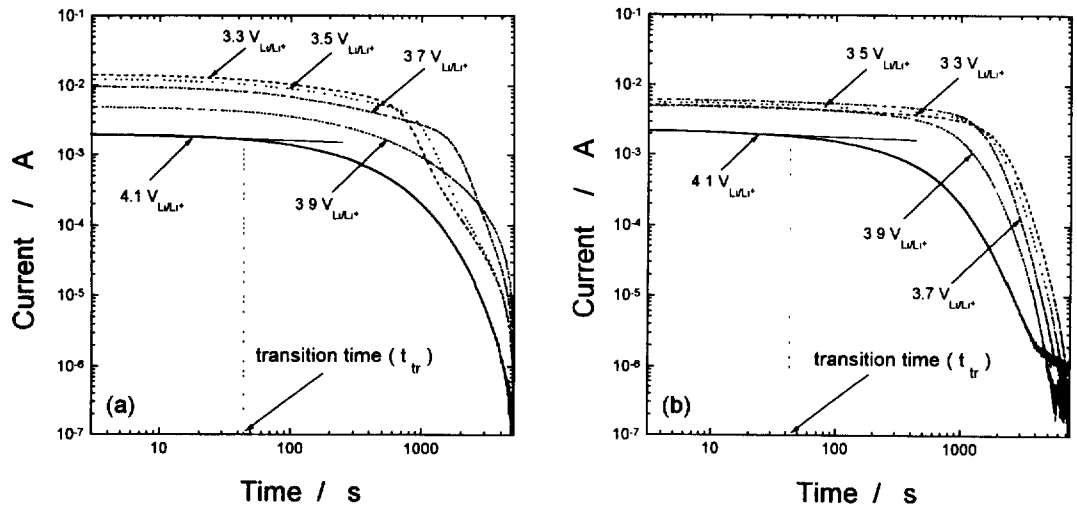

Fig. 3. Plots of (a) potentiostatic cathodic and (b) anodic current vs. time obtained from the porous $LiCoO_2$ electrode in 1 M $LiClO_4$/PC at 25 °C.

interface increased. By contrast, during the lithium de-intercalation t_{tr} increased as the lithium charging potential decreased, as presented in Fig. 3(b). The transition time t_{tr} can be theoretically defined as

$$t_{tr} = \frac{l^2}{\pi \tilde{D}_{Li^+}} \quad (1)$$

where $\tilde{D}_{Li^+}$ is the chemical diffusivity of the lithium ion and l represents the radius of the oxide particle. Provided that the lithium ion diffuses through a single phase, t_{tr} is constant, irrespective of the lithium charging potential [18]. Hence, the variation in t_{tr} with decreasing lithium charging potential cannot be accounted for in terms of diffusion in a single phase.

Assuming that the lithium-ion transport during the lithium intercalation proceeds by the movement of boundary between the concentrated β-phase and the dilute α-phase, and that the movement of phase boundary is very facile where the rate is determined by the diffusivity in the outer concentrated β-phase, then the cathodic intercalation current can be expressed as a function of time given in Eq. (2) in the initial stage of diffusion and Eq. (3) in the later stage [19]

$$I(t) = \frac{Q\sqrt{\tilde{D}_{Li^+,app}}}{l\sqrt{\pi}} t^{-1/2} \qquad t \ll \frac{l^2}{\tilde{D}_{Li^+,app}} \quad (2)$$

and

$$I(t) = \frac{2Q\tilde{D}_{Li^+,\beta}}{l^2} \exp\left(-\frac{\pi^2 \tilde{D}_{Li^+,\beta}}{4l^2} t\right) \qquad t \gg \frac{l^2}{\tilde{D}_{Li^+,app}} \quad (3)$$

where $I(t)$ is the current as a function of time, Q the total charge transferred during the electrochemical lithium intercalation($\int_0^\infty I(t)dt$), $\tilde{D}_{Li^+,app}$ the apparent chemical diffusivity of lithium ion, $\tilde{D}_{Li^+,\beta}$, the chemical diffusivity of the lithium ion in the concentrated β-phase, and t represents the time. Furthermore, t_{tr} can be given by

$$t_{tr} = \frac{l^2}{K_{mb}} \quad (4)$$

where K_{mb} is a constant associated with the apparent chemical diffusivity $\tilde{D}_{Li^+,app}$ and the concentration gradient over the more concentrated β-phase. The velocity of the phase boundary depends on the surface concentration of the oxide particles. During lithium intercalation, the lithium-concentrated β-phase is distributed not across the whole thickness of the oxide electrode but only over the relatively narrow region near the electrode surface. As the lithium charging potential decreases, the lithium concentration at the electrolyte/oxide electrode interface increases and, hence, the concentration gradient across the outer concentrated β-phase rises. The raised concentration gradient helps the phase boundary movement and thereby reduces t_{tr}. Therefore, this suggests that the lithium-ion transport during the intercalation proceeds not by the diffusion in a single phase but by the diffusion-controlled movement of the boundary between the α- and β-phases.

Recognizing that K_{mb} equals to $\pi\tilde{D}_{Li^+,app}$, the apparent chemical diffusivities $\tilde{D}_{Li^+,app}$ of lithium ion in the porous oxide electrode were determined by using Eq. (4) from the transition time t_{tr} on the cathodic intercalation and anodic de-intercalation current transients presented in Fig. 3 and the average particle size (particle diameter ≈ 20 μm, particle radius $l \approx 10$ μm) determined by the scanning electron microscopy (SEM). The determined apparent chemical diffusivities during lithium intercalation and de-intercalation are presented as a function of the lithium charging potential in Fig. 4.

The apparent chemical diffusivity $\tilde{D}_{Li^+,app}$ of the lithium ion in the porous oxide electrode was found to be (10^{-9}–10^{-8}) $cm^2\,s^{-1}$ at room temperature. During lithium de-intercalation, the apparent chemical diffusivity decreased with decreasing lithium charging potential. This tendency is similar to that charging potential dependence of the chemical diffusivity reported earlier by using galvanostatic intermittent titration technique (GITT) [16] and electrochemical impedance spectroscopy (EIS) [20]. According to our previous work [20], the diffusion of the lithium ion through layered transition metal oxides is not influenced by the change in interlayer spacing, but by the number of the vacant sites available for the lithium ion within the lithium-ion layer. With a decreasing lithium charging potential, the lithium content in the oxide is increased and, hence, the apparent chemical diffusivity of the lithium ion decreased. It is expected that a greater amount of the β-phase with a relatively low chemical diffusivity is formed over the oxide electrode as the lithium charging potential is lowered. Thus, the lithium-ion transport through the oxide electrode during the lithium de-intercalation is conceivably rate-controlled by the slowest step, the diffusion of the lithium ion in the β-phase rather than the movement of the phase boundary.

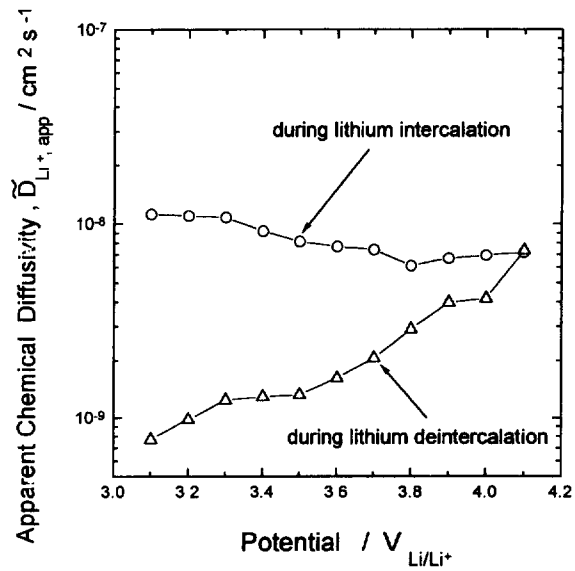

Fig. 4. Apparent chemical diffusivities $\tilde{D}_{Li^+,app}$ of the lithium ion in a porous $LiCoO_2$ electrode vs. lithium charging potential during the lithium intercalation and de-intercalation at 25 °C.

On the other hand, it is reasonable to state that the rate-determining step for the lithium-ion transport during the lithium intercalation is the phase-boundary movement rather than the diffusion of lithium ion in the β-phase. The reason why the lithium-ion transport proceeds by the phase boundary movement can be accounted for in the following way. The intercalation of the lithium ion is accompanied by the displacement of atoms constituting the oxide lattice and thereby build-up of a stress field in the lattice. When the abrupt potential drop of 500 to 1100 mV is applied to the oxide electrode, the steep concentration gradient is expected to be established near the surface region of the oxide particle. The steeper the concentration gradient is developed, the larger is the intercalation-induced stress gradient generated. On account of the large intercalation-induced stress gradient, the lithium-ion concentrated β-phase nucleates near the surface of the oxide particle and grows towards the center of the oxide particle [21]. Since the interaction energy of intercalated ions due to the elastic strain is inversely proportional to the volume of the intercalation electrode materials [22], the smaller the particle size, the larger is the effect of stress field gradient on the lithium-ion transport during the intercalation.

The quantitative analysis of the role of intercalation-induced stress in the lithium-ion transport through the oxide electrode with respect to the particle size of the oxide powder will be detailed in the following work [23].

4. Conclusions

The present work concerned the lithium-ion transport through the porous $LiCoO_2$ electrode by using cyclic voltammetry, charge/discharge experiments and potentiostatic current transient techniques. From the experimental results, the following conclusions are drawn:

1. The markedly strong reduction and oxidation current peaks observed at 3.90 and 4.05 V_{Li/Li^+}, respectively, are due to the intercalation into and de-intercalation of the lithium ion from only octahedral sites in the layered oxide structure. As against, the two weak current peaks encountered at 4.28 and 4.31 V_{Li/Li^+} higher than the intercalation/de-intercalation peak are related to an order/disorder phase transition arising at the $(1-\delta)$ range from 0.45 to 0.5 in $Li_{1-\delta}CoO_2$.
2. At the lithium charging potentials greater than or equal to the plateau potential in the charge/discharge curve, the cathodic current transients consist of two stages: (i) the diffusion of the lithium ion through the $Li_{1-\delta}CoO_2$ electrode, and (ii) the accumulation of lithium ion at the center of the oxide particle. This is valid only for the lithium charging potential region where a great portion of lithium gets over the intercalation/de-intercalation. The transition time from the first to second stage decreased with decreasing lithium charging potential. This suggests that the lithium-ion transport during the intercalation proceeds not by the diffusion in a single phase, but by the diffusion-controlled movement of boundary between the concentrated β-phase and the dilute α-phase.
3. The apparent chemical diffusivity $\tilde{D}_{Li^+,app}$ of the lithium ion in the porous $Li_{1-\delta}CoO_2$ electrode was determined to be $(10^{-9}$–$10^{-8})$ $cm^2\ s^{-1}$ at room temperature. With decreasing lithium charging potential, the apparent chemical diffusivity decreased monotonously during the lithium de-intercalation, but it increased during the lithium intercalation. The raised diffusivity value is ascribed to the phase-boundary movement caused by the intercalation-induced stress gradient generated across the α/β-phase boundary during the lithium intercalation.

Acknowledgements

The receipt of research grant under the University Foundation Research Program 'Development of High Performance Rechargeable Lithium Battery for Telecommunication Applications 1995/1996' from the Ministry of Information and Communication, Korea is gratefully acknowledged. Incidentally this paper was supported in part by Non-Directed Research Fund (1995/1996), Korea Research Foundation.

References

[1] K.M. Abraham, J.L. Goldman and M.D. Dempsy, *J. Electrochem. Soc., 128* (1981) 2493–2501.
[2] G. Pistoia, M. Pasqual, M. Tocci, R.V Moshtev and V. Maner, *J Electrochem. Soc., 130* (1985) 281–284.
[3] K West, B. Zachau-Christiansen, T. Jacobsen and S Atlung, *J. Power Sources, 14* (1985) 235–245.
[4] M. Lazzari and B. Scrosati, *J. Electrochem Soc., 127* (1980) 349–350.
[5] K. Mizushima, P C. Jones, P.J. Wiseman and J.B. Goodenough, *Mater. Res Bull., 15* (1980) 783–789.
[6] J.R. Dahn, U. von Sacken, M.W. Juzkow and H. Al-Janaby, *J. Electrochem. Soc., 138* (1991) 2207–2211.
[7] C. Delmas and I. Saadoune, *Solid State Ionics, 53* (1992) 370–375.
[8] M.M. Thackeray, P.J. Johnson, L.A de Picciotto, P.G. Bruce and J.B. Goodenough, *Mater Res. Bull., 19* (1984) 179–187.
[9] S. Bach, J.P. Pereira-Ramos, N. Baffier and R Messina, *J. Electrochem. Soc., 137* (1987) 1042–1047.
[10] N. Kumagai, I. Ishiyama and K. Tanno, *J. Power Sources, 20* (1987) 193–198
[11] J Scarmino, A. Talledo, A.A Andersson, S Passerini and F. Decker, *Electrochim. Acta, 38* (1993) 1637–1642.
[12] E. Rossen, J N Reimers and J R. Dahn, *Solid State Ionics, 62* (1993) 53–60.
[13] T. Ohzuku and A. Ueda, *J. Electrochem. Soc., 141* (1994) 2972–2977.
[14] R.J. Gummow and M.M. Thackeray, *Solid State Ionics, 53* (1992) 681–687.
[15] J N Reimers and J R. Dahn, *J. Electrochem Soc., 139* (1992) 2091–2097
[16] Y.-M. Choi, S.-I. Pyun, J.-S. Bae and S.-I. Moon, *J. Power Sources, 56* (1995) 25–30.

[17] J.-S. Bae and S.-I. Pyun, *Solid State Ionics, 90* (1996) 251–260.
[18] Y.-G. Yoon and S.-I. Pyun, *Electrochim. Acta*, (1997) in press.
[19] J. Crank, *The Mathematics of Diffusion*, Clarendon Press, Oxford, 1975, pp. 286–325.
[20] Y.-M. Choi, S.-I. Pyun and S.-I. Moon, *Solid State Ionics, 89* (1996) 43–52.
[21] T.-H. Yang, S.-I. Pyun and Y.-G. Yoon, *Electrochim. Acta, 42* (1997) 1701–1708.
[22] W.R. McKinnon and R.R. Haering, in R.E. White, J.O'M. Bockris and B.E. Conway (eds.), *Modern Aspects of Electrochemistry*, Vol. 15, Plenum, New York, 1983, pp. 235–304.
[23] Y.-M. Choi and S.-I. Pyun, *Solid State Ionics, 7* (1997) in press.